Protein synthesis persists during necrotic cell death

Xavier Saelens,[1] Nele Festjens,[1] Eef Parthoens,[2] Isabel Vanoverberghe,[1] Michael Kalai,[1] Frank van Kuppeveld,[3] and Peter Vandenabeele[1]

[1]Molecular Signalling and Cell Death Unit and [2]Microscopy Core Facility, Department for Molecular Biomedical Research, Flanders Interuniversity Institute for Biotechnology (VIB) and Ghent University, B9052 Ghent, Belgium
[3]Department of Medical Microbiology, Radboud University Nijmegen Medical Centre, 6500 HB Nijmegen, Netherlands

Cell death is an intrinsic part of metazoan development and mammalian immune regulation. Whereas the molecular events orchestrating apoptosis have been characterized extensively, little is known about the biochemistry of necrotic cell death. Here, we show that, in contrast to apoptosis, the induction of necrosis does not lead to the shut down of protein synthesis. The rapid drop in protein synthesis observed in apoptosis correlates with caspase-dependent breakdown of eukaryotic translation initiation factor (eIF) 4G, activation of the double-stranded RNA-activated protein kinase PKR, and phosphorylation of its substrate eIF2-α. In necrosis induced by tumor necrosis factor, double-stranded RNA, or viral infection, de novo protein synthesis persists and 28S ribosomal RNA fragmentation, eIF2-α phosphorylation, and proteolytic activation of PKR are absent. Collectively, these results show that, in contrast to apoptotic cells, necrotic dying cells retain the opportunity to synthesize proteins.

Introduction

Cell death is an essential part of metazoan development, homeostasis, and mammalian immune regulation. Based on the typical morphological features that become apparent in the course of cellular demise, three major types of cell death have been discerned: apoptosis, autophagic cell death, and necrosis (Schweichel and Merker, 1973; Clarke, 1990). The characteristic features of apoptosis, such as blebbing of the cell membrane, condensation of the nucleus, and internucleosomal cleavage of DNA, are a direct or indirect consequence of the activation of caspases (Hengartner, 2000; Lamkanfi et al., 2002). Autophagic cell death is characterized by extensive autophagy and appears in development as well as in pathological conditions such as Parkinson's disease and muscle diseases (Levine and Klionsky, 2004). The most prominent feature of necrosis is swelling (oncosis) of the cell and its organelles followed by loss of cell membrane integrity. Necrosis has often been considered as a passive process, lacking underlying signaling events. This assumption might hold for cell death resulting from severe physical or environmental damage such as hyperthermia or dounce- and detergent-induced lysis. However, necrotic cell death also occurs in normal physiological settings such as intestinal epithelium homeostasis (Barkla and Gibson, 1999). Necrosis is observed in various pathophysiological conditions such as cardiac ischemia and diseases associated with neuronal cell death such as stroke, amyotrophic lateral sclerosis, and Alzheimer's, Huntington's, and Parkinson's diseases (Colbourne et al., 1999; Nicotera et al., 1999). Furthermore, when caspase activation is prevented, necrosis can substitute for canonical caspase-dependent apoptosis induced by, for example, TNF, TNF-related apoptosis-inducing ligand, Fas ligand, and double-stranded RNA (dsRNA; Vercammen et al., 1998; Kalai et al., 2002; Vanden Berghe et al., 2003) and during digit formation in the developing mouse embryo (Chautan et al., 1999).

Convincing evidence for the existence of a programmed necrotic pathway was reported by Holler et al. (2000), who demonstrated that death domain receptor–induced necrosis of human T lymphocytes requires functional receptor interacting serine/threonine protein kinase 1 (RIP1). Dimerization of Fas-associated death domain (FADD) induces necrosis in caspase-8–deficient Jurkat T cells (Kawahara et al., 1998) and in the mouse L929 fibrosarcoma cell line in a RIP1-dependent way (Vanden Berghe et al., 2004). In line with this finding, RIP1- and FADD-deficient mouse embryonic fibroblasts prove resistant to necrosis induced by TNF in the presence of the pan-caspase inhibitor benzyloxycarbonyl-Val-Ala-DL-Asp(OMe)-fluoromethylketone (zVAD-fmk; Lin et al., 2004). Nevertheless, insight in the molecular events that operate during necrosis is still limited.

Correspondence to Peter Vandenabeele: Peter.Vandenabeele@dmbr.UGent.be

M. Kalai's present address is Unit of Molecular Microbiology, Institute Pasteur of Brussels, B1180 Brussels, Belgium.

Abbreviations used in this paper: CHX, cycloheximide; CVB, coxsackievirus B; dsRNA, double-stranded RNA; eIF, eukaryotic translation initiation factor; FADD, Fas-associated death domain; JE, Jurkat E; PARP, poly(ADP-ribose) polymerase; PI, propidium iodide; PKR, dsRNA-activated protein kinase; RIP1, receptor interacting serine/threonine protein kinase 1; ROS, reactive oxygen species; rRNA, ribosomal RNA; zVAD-fmk, benzyloxycarbonyl-Val-Ala-DL-Asp(OMe)-fluoromethylketone.

The online version of this article includes supplemental material.

The Journal of Cell Biology, Vol. 168, No. 4, February 14, 2005 545–551
http://www.jcb.org/cgi/doi/10.1083/jcb.200407162

Induction of apoptosis is characterized by a general inhibition of protein synthesis that is attributed to the proteolytic attack of translation initiation factors (Clemens et al., 2000). Because the effect of necrotic cell death on the translational machinery has not been examined, we compared the protein synthesis capacity of cells subjected to apoptotic or necrotic death stimuli. We show that after necrosis, protein synthesis is sustained in the dying cell, up to the point where the cell loses its membrane integrity.

Results and discussion

dsRNA and TNF induce necrosis in Jurkat T cell clones

To test if protein synthesis is disturbed during a necrotic response, we made use of three different Jurkat T cell lines. Wild-type cells (Jurkat E [JE]) respond to Fas-ligation by apoptosis and were used as control. As a first model of necrosis we chose dsRNA treatment of JB6 cells. These cells, genetically deficient in caspase-8 and overexpressing Bcl-2, die in a necrotic way in response to dsRNA, unlike JE cells, which hardly respond to dsRNA (Kalai et al., 2002). In a second model, we used death receptor–induced necrosis of FADD-deficient cells stimulated with TNF (TNF was used because, in our hands, Fas-ligation in the absence of caspase-8 or FADD or in the presence of caspase inhibitors barely induced necrosis). As expected, JE cells treated with agonistic anti-Fas antibody displayed blebbing of the cell membrane and little or no propidium iodide (PI) staining at the early stage of apoptosis (Fig. 1 A). Treatment of JB6 cells with dsRNA or of FADD-deficient cells with TNF induced swelling of the cells, followed by cellular collapse and loss of membrane integrity. To further differentiate between cell death types, the generation of reactive oxygen species (ROS) was assessed. An increase in ROS production was detected starting 2–4 h after stimulation in necrotic but not in apoptotic cells (Fig. 1 B). Finally, the caspase inhibitors zVAD-fmk and qVD-OPH failed to prevent necrotic cell death (Fig. 1 C).

The rate of protein synthesis remains constant during necrosis

To compare de novo protein synthesis in the course of apoptosis and necrosis, cells were pulse-labeled with ^{35}S-methionine at various time points after induction of cell death. In agreement with previous reports, induction of apoptosis in JE cells resulted in a rapid decrease in de novo protein synthesis that was already apparent 2 h after treatment with agonistic anti-Fas antibody (Fig. 2 A and Fig. S1, available at http://www.jcb.org/cgi/content/full/jcb.200407162/DC1). In contrast, the rate of protein synthesis in JB6 cells treated with dsRNA and in FADD-deficient cells exposed to TNF was not affected up to 8 h after treatment, when the majority of the cells had already lost membrane integrity. The kinetics of cell death, determined by the loss of membrane integrity, were similar in the apoptotic and necrotic settings (Fig. 2 A). We conclude that necrosis induced by dsRNA or TNF in Jurkat cells does not affect the overall protein synthesis capacity of the cells destined to die. Pulse-labeling experiments of mouse L929 cells stimulated to

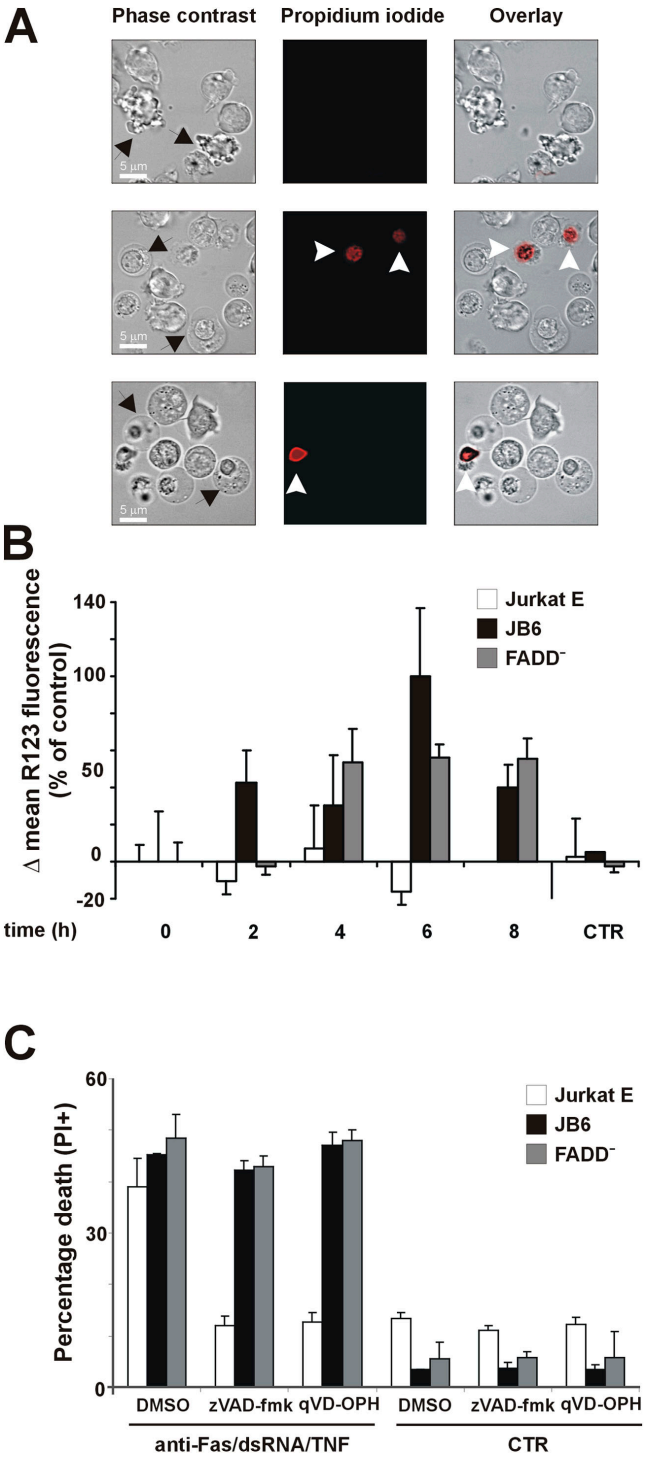

Figure 1. **dsRNA and TNF induce necrosis in JB6 and FADD-deficient Jurkat cells.** (A) Microscopic analysis. JE cells were treated with anti-Fas antibody to induce apoptosis (top), JB6 cells with dsRNA (middle), and FADD-deficient cells with TNF (bottom). Photomicrographs were taken after 4 (JE) and 6 h (JB6 and FADD-deficient cells). Apoptotic cells showing blebbing of the cell membrane and necrotic cells displaying swelling are indicated (closed arrows). In the middle and right columns, cells with nuclear PI staining are indicated with open arrowheads. (B) Cells were treated with anti-Fas (JE), dsRNA (JB6), or TNF (FADD$^-$) or left untreated (CTR) for the indicated time periods. ROS production was determined by measuring the fluorescence intensity of rhodamine 123 in PI-negative cells. Bars represent mean values from three experiments, relative to time 0 (set to 100%). (C) Cells, pretreated for 30 min with 25 μM zVAD-fmk, quinoline-Val-Asp-O-phenoxy (q-VD-OPH), or DMSO, were stimulated with anti-Fas (JE), dsRNA (JB6), or TNF (FADD$^-$) for 8 h. Control (CTR) cells were not stimulated. Error bars equal SD of the mean (n = 3).

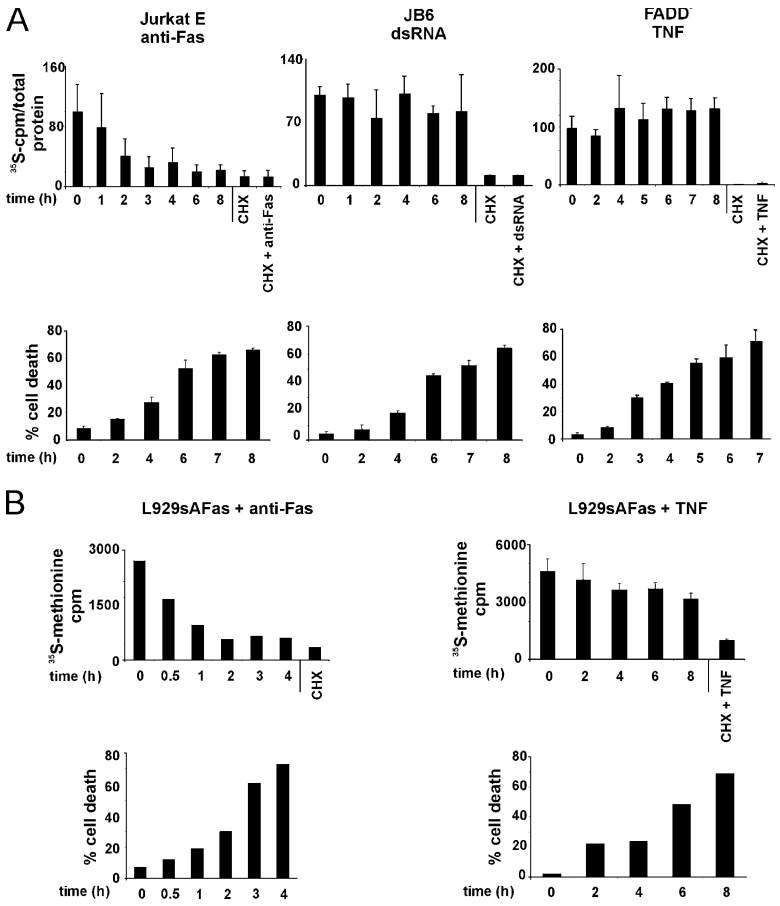

Figure 2. **Translation is rapidly shut down in apoptosis but not in necrosis.** (A) Protein synthesis in Jurkat cells was analyzed by pulse-labeling cells for 30 min with 10 μCi ^{35}S-methionine in normal medium at various time points after stimulation. Pulse-labeling was also performed on unstimulated cells treated for 1 h with 10 μg/ml CHX and on cells stimulated for 6 h with anti-Fas, dsRNA, or TNF together with CHX added 1 h before addition of ^{35}S-methionine. After labeling, cells were lysed and 30-μg samples were resolved by SDS-PAGE followed by Coomassie staining and autoradiography. Coomassie and radioactivity signals from gels were quantified by densitometry and phosphorimaging, respectively, and the ratio of ^{35}S-counts over total protein in each lane was calculated (top). Cell death from cells used for pulse-labeling experiments was determined by trypan blue exclusion (bottom). (B) The rate of protein synthesis remains constant during TNF-induced necrosis in mouse L929 fibrosarcoma cells. L929sAFas cells were seeded at 2.5×10^5 cells/ml in suspension plates on the day before labeling with ^{35}S-methionine. 30-min pulse-labeling was performed at different time points after stimulation with 100 ng/ml anti-Fas (left) or 5,000 IU/ml TNF (right) to induce apoptosis and necrosis, respectively (top). CHX (10 μg/ml; 1 h)-treated cells were also included. Cell lysates were prepared and analyzed by measuring scintillation counts of TCA-precipitated cell extracts (anti-Fas–treated cells) or by SDS-PAGE followed by Coomassie staining and autoradiography (TNF-treated cells). ^{35}S scintillation counts of anti-Fas–treated cells are depicted (left). For TNF-treated cells, ^{35}S counts in each lane of the gels were quantitated using a phosphorimager and represented as mean values from three independent experiments (right). Cell death in the same experiment was monitored by trypan blue exclusion (bottom). Data in A and B represent mean values and error bars indicate the SD of the mean ($n = 3$).

die necrotically or apoptotically confirmed that the rate of protein synthesis is not overtly affected in necrosis, whereas translation is rapidly shut down in apoptosis (Fig. 2 B).

The protein synthesis machinery remains intact during necrosis

The initiation phase of protein synthesis constitutes the major site of its regulation. Eukaryotic translation initiation factor (eIF) 4G is a prime determinant in eukaryotic translation initiation because it provides the molecular bridge between the mRNA and the ribosome (Pestova et al., 2001). Caspase-dependent as well as caspase-independent cleavage of eIF4G has been reported and this event correlates with the shut down of protein synthesis (Clemens et al., 2000). Because protease activity may contribute to necrosis, we assessed the integrity of eIF4G by immunoblotting. In cells treated with anti-Fas, a 45-kD fragment of eIF4G was clearly detected (Fig. 3 A). In contrast, no generation of eIF4G fragments in dsRNA- or TNF-induced necrosis was found. Next, we examined the modification of translation initiation factor eIF2-α in apoptotic and necrotic cells. eIF2-α is a subunit of the heterotrimeric eukaryotic translation initiation factor eIF2, which mediates the binding of initiator Met-tRNAi to the 40S ribosomal subunit. eIF2-α phosphorylation leads to translation inhibition and in apoptosis coincides with caspase-dependent cleavage and activation of the eIF2-α kinase dsRNA-activated protein kinase (PKR; Saelens et al., 2001). eIF2-α phosphorylation increased 2 h after anti-Fas treatment, coinciding with eIF4G cleavage, PKR cleavage, and the drop in the rate of translation (Figs. 2 A and 3 A). No PKR cleavage or significant eIF2-α phosphorylation was observed in either necrotic system. DsRNA is a potent activator of PKR, and extracellularly administered poly-inosinic-cytidylic acid can activate PKR in a TRIF (TIR domain-containing adaptor inducing IFN-β)-dependent manner (Hsu et al., 2004). The lack of PKR activation in JB6 cells exposed to dsRNA is somewhat surprising. It is possible that the TLR3 pathway in JB6 cells, which have a strong antiapoptotic constellation (overexpression of Bcl-2 and lack of caspase-8), favors RIP1-mediated necrosis (Kalai et al., 2002), a condition that may interfere with PKR activation.

Cleavage of 28S ribosomal RNA (rRNA) in a caspase-dependent or -independent way has been shown to correlate with inhibition of protein synthesis in cell death, and therefore was also analyzed (Houge et al., 1995). Apoptotic cells displayed two distinct RNA bands reportedly derived from 28S rRNA (Fig. 3 B; Houge et al., 1995). In contrast, the induction of necrosis by dsRNA treatment of JB6 cells and by TNF treatment of FADD-deficient cells did not generate detectable rRNA alterations, which is in line with the ability of the cell to maintain protein synthesis (Fig. 3 B).

Necrosis in wild-type Jurkat cells

To ascertain the physiological relevance of necrosis in wild-type JE, we monitored cell death induced by a nonenveloped, cytolytic virus. We found that coxsackievirus B (CVB), an en-

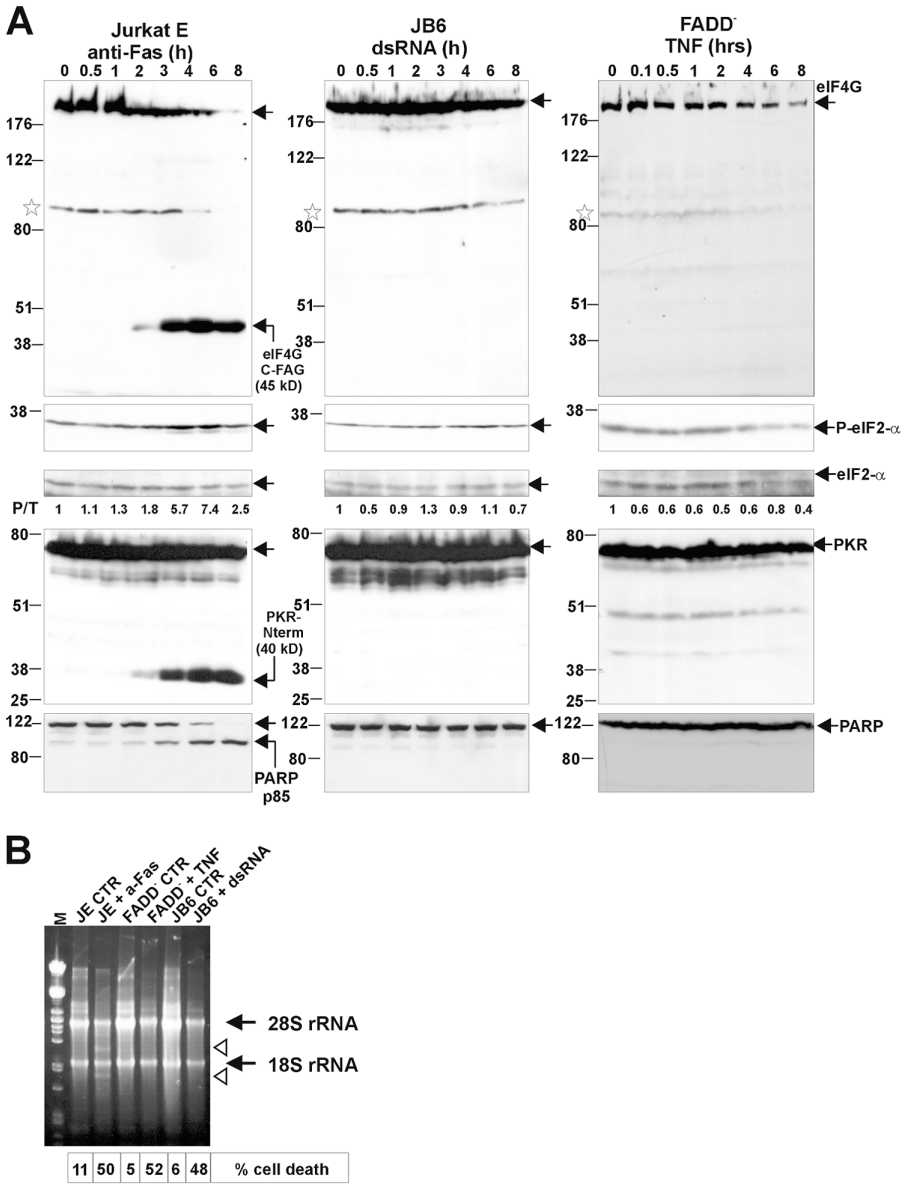

Figure 3. **Translation initiation factors eIF4G, eIF2-α, PKR, and PARP remain intact in necrosis but not in apoptosis.** (A) Western blot analysis of total cell lysates reveals the cleavage of eIF4G into a 45-kD fragment (eIF4G C-FAG) in time after anti-Fas treatment of JE cells (left). Asterisks denote an aspecific band. The phosphorylation status of eIF2-α was monitored using an antibody specific for eIF2-α phosphorylated at Ser51 (P-eIF2-α). The total amount of eIF2-α was also assessed on the same blot after inactivation of the P-eIF2-α signal by overnight treatment of the blot with 0.1% NaN_3. The ratio of phosphorylated over total eIF2-α signal per lane was determined by densitometric analysis, normalized to 1 for time 0, and is indicated below each lane. Immunoblots for PKR and PARP show the appearance of a 40-kD PKR fragment (PKR-Nterm) and of an 85-kD fragment of PARP in apoptosis. (B) Ribosomal 28S RNA is cleaved in apoptosis but not in necrosis. 10 μg of total RNA isolated from cells treated as indicated was analyzed by agarose gel electrophoresis followed by ethidium bromide staining. Arrows indicate the position of 28S and 18S rRNA. Arrowheads indicate cleavage products in the anti-Fas–treated sample. CTR, untreated.

terovirus belonging to the *Picornaviridae* family, induces necrosis-like cell death in both JE and JB6 cells. CVB replicated efficiently in both cell lines and induced swelling of the cells followed by loss of membrane integrity (Fig. 4, A and B). Virus-induced cell death, which became apparent 6 h after infection, proceeded without caspase activity or poly(ADP-ribose) polymerase (PARP) cleavage (Fig. 4, C, D, and F). CVB infection had little, if any, effect on protein synthesis in both cell lines (Fig. 4 E). eIF4G analysis showed the generation of a 100-kD COOH-terminal fragment (Fig. 4 F), an event that is typically observed in enterovirus-infected cells (Etchison et al., 1982) and that has been implicated in the virus-induced switch from cap-dependent host cell translation to IRES-driven translation of the viral genome (Ehrenfeld, 1982). The morphology of the dying cells and the absence of caspase activation strongly indicate that even apoptosis-competent cells can die by necrosis, e.g., following a viral infection. Finally, we also analyzed the effect of an apoptotic and a necrotic stimulus on CVB replication. We found that anti-Fas treatment of infected JE cells suppresses translation and viral progeny by 10-fold (Fig. 5, A and C). In contrast, enhancing necrosis by dsRNA treatment of infected JB6 cells did not affect translation or CVB propagation (Fig. 5, B and D). This finding provides evidence that CVB can efficiently propagate in translationally active cells dying of necrosis but not in apoptotic cells in which protein synthesis is blocked.

Physiological implications of ongoing translation in necrosis

Our results demonstrate that necrosis induced by dsRNA or TNF treatment of Jurkat T lymphocytes and by TNF in L929 fibrosarcoma cells does not affect the protein synthesis rate. DsRNA and TNF give rise to a rapid and strong induction of gene expression as evidenced by the phosphorylation status of p38 MAPK (unpublished data). In a cell destined to die by necrosis, translation of newly synthesized transcripts could still occur, resulting for example in gene products that may alert other cells in a local or

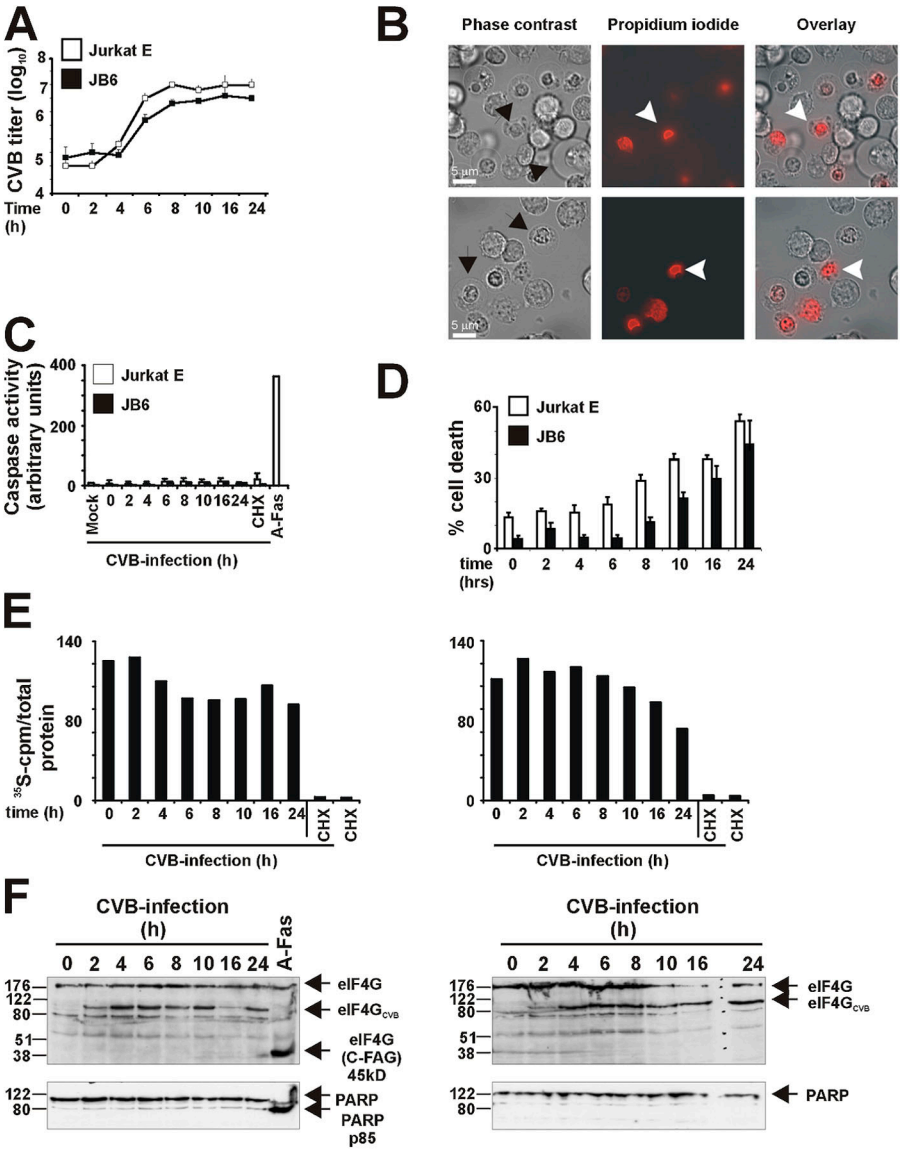

Figure 4. **Coxsackievirus induces necrosis-like death.** Cells were infected with CVB (multiplicity of infection of 20) for 1 h, washed, and incubated for the time points indicated. (A) CVB replicates in JE and JB6 cells. Y-axis shows virus titer (in 50% tissue culture infective dose/ml). (B) Microscopic analysis of JE (top) and JB6 (bottom) cells infected with CVB for 16 h. Closed arrows indicate swollen cells; open arrowheads indicate cells with nuclear PI staining. (C) Jurkat cells do not display caspase activity following CVB infection. As a control, a sample from anti-Fas–treated JE cells was also analyzed (A-Fas). (D) Kinetics of cell death following CVB infection of JE and JB6 cells, as measured by permeability to trypan blue. (E) Translation rate of JE (left) and JB6 (right) cells infected in D. Coomassie and radioactivity signals from SDS-PAGE gels were quantified by densitometry and phosphorimaging, respectively, and the ratio of ^{35}S-counts over total protein in each lane were calculated. Data in the graph are from one experiment that was performed three times, giving similar results. (F) Fate of eIF4G (top) and PARP (bottom) in CVB-infected JE (left) and JB6 (right) cells. Note that eIF4G is not cleaved into the apoptotic 45-kD fragment, but, instead, into a 100-kD fragment (eIF4G$_{CVB}$). A-Fas, apoptotic lysates.

systemic fashion. Apoptosis is often considered as a "clean death" because it prevents the release of the intracellular content of the cell. Rapid inhibition of translation may contribute to keep apoptotic cell demise immunologically silent. Moreover, apoptosis can be considered as an antiviral host cell response aimed at curtailing virus replication. In contrast, necrotic cell death and spilling of the intracellular content into the extracellular environment can trigger inflammation by providing "danger" signals for the surrounding cells and immune competent cells, such as dendritic cells, granulocytes, and monocytes (Sauter et al., 2000). However, at the same time, viruses, which often use strategies to modulate the apoptotic program, may profit from the available translation apparatus in the necrotic cell to propagate until the cell eventually demises.

Materials and methods

Cell culture and induction of apoptosis or necrosis

Jurkat T cells were grown as described previously (Kalai et al., 2002). Parental E cells and JB6 cells were provided by S. Nagata (Osaka University Medical School, Osaka, Japan). FADD-deficient cells were provided by J. Blenis (Harvard Medical School, Boston, MA). 100 ng/ml CH-11 anti-Fas antibody (BioCheck) was used to induce apoptosis in JE cells. 50 μg/ml dsRNA (poly (I)-poly(C)) (Amersham Biosciences) and 5000 IU/ml of human TNF were used to induce necrosis in JB6 and FADD-deficient cells, respectively. Caspases were blocked by incubating cells for 30 min with 25 μM zVAD-fmk (Bachem) or quinoline-Val-Asp-O-phenoxy (MP Biomedicals) before stimulation. Cell death was monitored by trypan blue exclusion or by measuring PI (15 μM) uptake at 610 nm by FACS analysis using a FACScalibur flow cytometer (Becton Dickinson) equipped with a 488-nm Argon laser. ROS production was measured as the fluorescence at 525 nm of rhodamine 123, resulting from oxidation of dihydrorhodamine 123 (Molecular Probes) in PI-negative cells. Dihydrorhodamine 123 was applied to the cells at 0.1 μM 30 min before analysis. Relative fluorescence values are depicted as the ratio between the fluorescent signal at a given time point and the initial fluorescence for the same condition, using mean fluorescence values from a representative experiment performed in triplicate. Caspase activity was determined as described using DEVD-amc as substrate (Saelens et al., 2001).

Microscopic analysis

Cells were seeded in normal growth medium in 8-chambered cover glass (Nunc) and treated for the time indicated in the legends of Figs. 1 and 4. Phase-contrast images and fluorescence images were photographed using a microscope (model DM IRE2; Leica) equipped with a HCX PLAPO 63×/1.30 glycerine corrected 37°C lens and a coolsnap HQ camera.

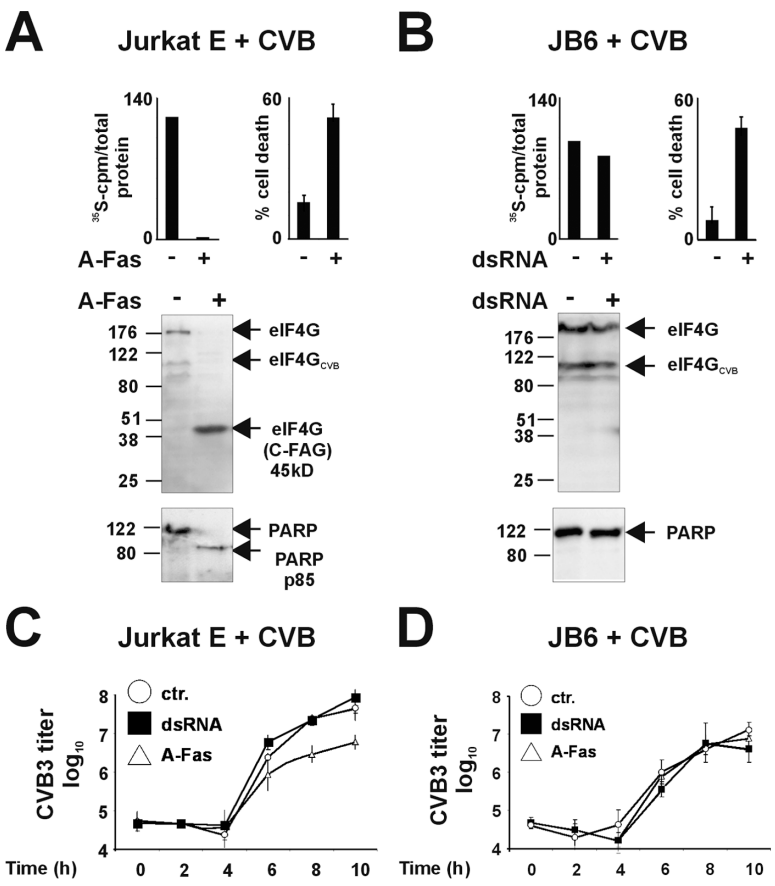

Figure 5. **Induction of apoptosis in CVB-infected cells leads to a drop in virus titer, whereas enhancing necrosis by dsRNA-treatment of infected JB6 cells does not affect virus propagation.** CVB-infected JE (A and C) or JB6 (B and D) cells were left untreated (−) or stimulated with anti-Fas or dsRNA, respectively, for 8 h, starting 2 h after infection. (A and B) Cells were pulse-labeled with ^{35}S-methionine, and the amount of incorporated ^{35}S in the protein fraction of cell lysates and cell death was determined (top). Effects on eIF4G and PARP were analyzed by immunoblotting (bottom). (C and D) CVB titers from JE (C) and JB6 (D) infected cells stimulated with anti-Fas or dsRNA or left untreated (ctr). Error bars equal SD of the mean (n = 3).

The camera is controlled by the ASMDW acquisition software (Leica). PI (1 μM) fluorescence was monitored at 540 nm using a 50-W Xe lamp for excitation. Blind deconvolution of the fluorescence and overlay images was performed using Metamorph 5.0 software.

Metabolic labeling of proteins

To avoid stress responses, metabolic labeling of the cells was performed in normal growth medium. 16 h before labeling, cells were seeded at 10^6 cells/ml. At selected time points after stimulation, samples of 1.5×10^6 cells were transferred to a 6-well plate and labeled for 30 min with 10 μCi of Trans^{35}S-label (MP Biomedicals). 10 μg/ml cycloheximide (CHX) was added to cells 1 h before labeling. After pulse labeling, cells were washed twice with ice-cold PBS and lysed on ice with caspase lysis buffer containing 10 mM Tris-HCl, pH 7.5, 200 mM NaCl, 5 mM EDTA, 10% glycerol, 1% NP-40, 1 mM aprotinin, 1 mM leupeptin, and 100 μM PMSF. From each time point, 30 μg of protein from the 14,000 *g* supernatant fraction was resolved by SDS-PAGE and visualized by Coomassie brilliant blue staining. The intensity of the Coomassie-stained bands in each lane was quantified by densitometry. After drying, ^{35}S signals from the gels were captured and quantified using a PhosphorImager (Bio-Rad Laboratories).

Immunoblot analysis

Protein extracts from cell lines were prepared by lysis with sample buffer, separated in 12.5% SDS-PAGE gels, and transferred to nitrocellulose. Antibodies against the following antigens were used to probe the blots: eIF4G and PKR (Transduction Laboratories), phosphorylated eIF2-α (Research Genetics), eIF2-α (Santa Cruz Biotechnology, Inc.), PARP (BIOMOL Research Laboratories, Inc.), phosphorylated-p38 MAPK (Biosource International), and total p38 MAPK (Cell Signaling Technology). Immuno-reactive proteins were visualized using chemiluminescence and signals were captured by exposure to film (Amersham Biosciences). Bands on the luminographs were quantitated by densitometry using a Lumi-Imager workstation (Roche Molecular Biochemicals).

Analysis of rRNA

6 and 7 h after induction of apoptosis and necrosis, total RNA was prepared using an RNeasy kit (QIAGEN). 10 μg of RNA was separated in an agarose gel, using Tris-Borate-EDTA as running buffer, and stained with ethidium bromide.

Viral infection

CVB used in this study was derived from plasmid pCB3/T7, containing a cDNA of coxsackievirus type B3 (strain Nancy) behind a T7 RNA polymerase promoter. Viruses were grown and titrated on Buffalo green monkey kidney cells. Jurkat cells were infected for 1 h at 37°C at a multiplicity of infection of 20 TCID50 (50% tissue culture infective dose) per cell. Hereafter, cells were washed and incubated at 37°C for further analysis at the indicated time periods. Viruses were extracted from the Jurkat cells by three cycles of freeze thawing and titrated on Buffalo green monkey kidney cells.

Online supplemental material

Fig. S1 shows that translation is rapidly shut down in apoptosis but not in necrosis. Online supplemental material is available at http://www.jcb.org/cgi/content/full/jcb.200407162/DC1.

We thank A. Bredan for editorial help. We are grateful to S. Nagata and J. Blenis for the caspase-8 and FADD-deficient Jurkat cells.

This work was supported by the Interuniversitaire Attractiepolen-V (IUAP-V), Fonds voor Wetenschappelijk Onderzoek-Vlaanderen (grants 3G.0006.01 and 3G.021199), Belgian Federation against Cancer, European Community Research, Technological Development and Demonstration (EC-RTD; grant QLG1-CT-1999-00739), Ghent University cofinancing EU project (011C0300), and Geconcerteerde Onderzoeksacties (GOA) project (12050502). X. Saelens is supported by GOA project 12050502, N. Festjens by Instituut voor de aanmoediging van Innovatie door Wetenschap en Technologie in Vlaanderen and IUAP-V, M. Kalai by EC-RTD, and F. van Kuppeveld by grants from the Netherlands Organization for Scientific Research (NWO-VIDI 917.46.305) and the Beijerink Premie (2004).

Submitted: 26 July 2004
Accepted: 30 December 2004

References

Barkla, D.H., and P.R. Gibson. 1999. The fate of epithelial cells in the human large intestine. *Pathology.* 31:230–238.

Chautan, M., G. Chazal, F. Cecconi, P. Gruss, and P. Golstein. 1999. Interdigital cell death can occur through a necrotic and caspase-independent pathway. *Curr. Biol.* 9:967–970.

Clarke, P.G. 1990. Developmental cell death: morphological diversity and multiple mechanisms. *Anat. Embryol. (Berl.).* 181:195–213.

Clemens, M.J., M. Bushell, I.W. Jeffrey, V.M. Pain, and S.J. Morley. 2000. Translation initiation factor modifications and the regulation of protein synthesis in apoptotic cells. *Cell Death Differ.* 7:603–615.

Colbourne, F., G.R. Sutherland, and R.N. Auer. 1999. Electron microscopic evidence against apoptosis as the mechanism of neuronal death in global ischemia. *J. Neurosci.* 19:4200–4210.

Ehrenfeld, E. 1982. Poliovirus-induced inhibition of host cell protein synthesis. *Cell.* 28:435–436.

Etchison, D., S.C. Milburn, I. Edery, N. Sonenberg, and J.W. Hershey. 1982. Inhibition of HeLa cell protein synthesis following poliovirus infection correlates with the proteolysis of a 220,000-dalton polypeptide associated with eucaryotic initiation factor 3 and a cap binding protein complex. *J. Biol. Chem.* 257:14806–14810.

Hengartner, M.O. 2000. The biochemistry of apoptosis. *Nature.* 407:770–776.

Holler, N., R. Zaru, O. Micheau, M. Thome, A. Attinger, S. Valitutti, J.L. Bodmer, P. Schneider, B. Seed, and J. Tschopp. 2000. Fas triggers an alternative, caspase-8-independent cell death pathway using the kinase RIP as effector molecule. *Nat. Immunol.* 1:489–495.

Houge, G., B. Robaye, T.S. Eikhom, J. Golstein, G. Mellgren, B.T. Gjertsen, M. Lanotte, and S.O. Doskeland. 1995. Fine mapping of 28S rRNA sites specifically cleaved in cells undergoing apoptosis. *Mol. Cell. Biol.* 15:2051–2062.

Hsu, L.C., J.M. Park, K. Zhang, J.L. Luo, S. Maeda, R.J. Kaufman, L. Eckmann, D.G. Guiney, and M. Karin. 2004. The protein kinase PKR is required for macrophage apoptosis after activation of Toll-like receptor 4. *Nature.* 428:341–345.

Kalai, M., G. Van Loo, T. Vanden Berghe, A. Meeus, W. Burm, X. Saelens, and P. Vandenabeele. 2002. Tipping the balance between necrosis and apoptosis in human and murine cells treated with interferon and dsRNA. *Cell Death Differ.* 9:981–994.

Kawahara, A., Y. Ohsawa, H. Matsumura, Y. Uchiyama, and S. Nagata. 1998. Caspase-independent cell killing by Fas-associated protein with death domain. *J. Cell Biol.* 143:1353–1360.

Lamkanfi, M., W. Declercq, M. Kalai, X. Saelens, and P. Vandenabeele. 2002. Alice in caspase land. A phylogenetic analysis of caspases from worm to man. *Cell Death Differ.* 9:358–361.

Levine, B., and D.J. Klionsky. 2004. Development by self-digestion: molecular mechanisms and biological functions of autophagy. *Dev. Cell.* 6:463–477.

Lin, Y., S. Choksi, H.M. Shen, Q.F. Yang, G.M. Hur, Y.S. Kim, J.H. Tran, S.A. Nedospasov, and Z.G. Liu. 2004. Tumor necrosis factor-induced nonapoptotic cell death requires receptor-interacting protein-mediated cellular reactive oxygen species accumulation. *J. Biol. Chem.* 279:10822–10828.

Nicotera, P., M. Leist, and L. Manzo. 1999. Neuronal cell death: a demise with different shapes. *Trends Pharmacol. Sci.* 20:46–51.

Pestova, T.V., V.G. Kolupaeva, I.B. Lomakin, E.V. Pilipenko, I.N. Shatsky, V.I. Agol, and C.U. Hellen. 2001. Molecular mechanisms of translation initiation in eukaryotes. *Proc. Natl. Acad. Sci. USA.* 98:7029–7036.

Saelens, X., M. Kalai, and P. Vandenabeele. 2001. Translation inhibition in apoptosis: caspase-dependent PKR activation and eIF2-alpha phosphorylation. *J. Biol. Chem.* 276:41620–41628.

Sauter, B., M.L. Albert, L. Francisco, M. Larsson, S. Somersan, and N. Bhardwaj. 2000. Consequences of cell death: exposure to necrotic tumor cells, but not primary tissue cells or apoptotic cells, induces the maturation of immunostimulatory dendritic cells. *J. Exp. Med.* 191:423–434.

Schweichel, J.U., and H.J. Merker. 1973. The morphology of various types of cell death in prenatal tissues. *Teratology.* 7:253–266.

Vanden Berghe, T., M. Kalai, G. Van Loo, W. Declercq, and P. Vandenabeele. 2003. Disruption of HSP90 function reverts tumor necrosis factor-induced necrosis to apoptosis. *J. Biol. Chem.* 278:5622–5629.

Vanden Berghe, T., G. van Loo, X. Saelens, M. van Gurp, G. Brouckaert, M. Kalai, W. Declercq, and P. Vandenabeele. 2004. Differential signaling to apoptotic and necrotic cell death by Fas-associated death domain protein FADD. *J. Biol. Chem.* 279:7925–7933.

Vercammen, D., G. Brouckaert, G. Denecker, M. Van de Craen, W. Declercq, W. Fiers, and P. Vandenabeele. 1998. Dual signaling of the Fas receptor: initiation of both apoptotic and necrotic cell death pathways. *J. Exp. Med.* 188:919–930.